

2 mix

CR-134151

SPACE SHUTTLE GN&C EQUATION DOCUMENT
 No. 14
 (Revision 1)
 Deorbit Targeting
 by
 Wayne H. Tempelman

(NASA-CR-134151) DEORBIT TARGETING
 (Draper (Charles Stark) Lab., Inc.)
 CSCL 22B N74-12513
 63/31 Unclass 23105

PRICES SUBJECT TO CHANGE

Reproduced by
 NATIONAL TECHNICAL
 INFORMATION SERVICE
 U.S. Department of Commerce
 Springfield, VA. 22151

CHARLES STARK DRAPER LABORATORY

MASSACHUSETTS INSTITUTE OF TECHNOLOGY

CAMBRIDGE, MASSACHUSETTS, 02139

27

SPACE SHUTTLE GN&C EQUATION DOCUMENT

No. 14

(Revision 1)

Deorbit Targeting

by

Wayne H. Tempelman

Charles Stark Draper Laboratory

June 1973

NAS9-10268

for

National Aeronautics and Space Administration

Guidance and Control Systems Branch

Avionics Systems Engineering Division

Lyndon B. Johnson Space Center, Houston, Texas

ACKNOWLEDGEMENT

This report was prepared under DSR Project 55-40800, sponsored by the Manned Spacecraft Center of the National Aeronautics and Space Administration through Contract NAS9-10268.

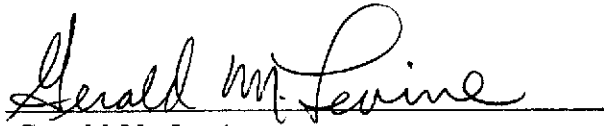
The publication of this report does not constitute approval by the National Aeronautics and Space Administration of the findings or the conclusions contained therein. It is published only for the exchange and stimulation of ideas.

REVISION 1 CHANGES

This document represents a substantial revision of the previous one dated October 1971. The major modification involves the use of the Unified Powered Flight Guidance Routine during the deorbit targeting to accurately estimate the effects of the finite thrust maneuvers for the low thrust/weight ratios associated with the Shuttle project.

FOREWORD

This document is one of a series of candidates for inclusion in a future revision of JSC -04217 "Space Shuttle Guidance, Navigation and Control Design Equations". The enclosed has been prepared under NAS9-10268, Task No. 15-A, "GN&C Flight Equation Specification Support", and applies to functions 1, 2, 4 and 5 of the Entry Guidance Module (OG5) as defined in JSC -03690, Rev. D, "Space Shuttle Orbiter Guidance, Navigation, and Control Software Functional Requirements", dated January 1973.

A handwritten signature in cursive script, reading "Gerald M. Levine", is written over a horizontal line.

Gerald M. Levine
Division Leader, Guidance Analysis
NASA Programs Department

TABLE OF CONTENTS

Section 1	Introduction
Section 2	Functional Flow Diagram
Section 3	Input and Output Variables
Section 4	Description of Equations
Section 5	Detailed Flow Diagrams
Section 6	Supplementary Information

NOMENCLATURE

a	Semi-major axis
a_F	Semi-major axis of Fischer ellipsoid
a_T	Estimated magnitude of thrust acceleration
b_F	Semi-minor axis of Fischer ellipsoid
c	Iteration counter
c_1, c_2	Constants in the v_r, v_h entry interface relationship
c_3	Constant in the thrust direction equation
d	Number of columns of navigation filter weighting matrix
d_{ACR}	Maximum acceptable crossrange distance
d_{CR}	Entry crossrange distance
f	Magnitude of the engine thrust
g_0	Reference value for the acceleration of gravity
h_{EI}	Entry interface altitude
\underline{i}	Unit vector specified by the cross product of the angular momentum and the landing site vector
\underline{i}_{EI}	Unit vector in the direction of \underline{r}_{EI}
\underline{i}_H	Unit vector in the direction of the angular momentum vector
\underline{i}_{LSP}	Unit vector in the direction of the landing site projection into the orbital plane

\underline{i}_N	Unit vector normal to the trajectory plane
m	Estimated vehicle mass
n	Number of guidance phases
n_{rev}	Integral number of complete revolution to be made in the transfer
p	Orbital period
\underline{r}_D	Position at the start of the deorbit maneuver
\underline{r}_{EI}	Entry interface position
\underline{r}_{LS}	Landing site position
\underline{r}_0	Input position and projected landing site position
\underline{r}_{OF}	Offset target vector
\underline{r}_{PEI}	Projected entry interface position
\underline{r}_{PLS}	Projected landing site position into the orbital plane
s_{fail}	Failure switch
s_{FP}	First pass switch
s_{mode}	Maneuver mode switch
$s_{OMS, 1}$	Number of orbital maneuvering system (OMS) engines
s_p	Precision mode switch
$s_{phase, 1}$	Phase switch
s_{pert}	Perturbation switch
s_{soln}	Lambert solution switch

t_D	Time at the start of the deorbit maneuver
t_{D0}	Value of t_D from previous iteration cycle
t_{EI}	Entry interface time
t_{ETL}	Desired earliest time-of-landing
t_{LTL}	Desired latest time-of-landing
t_0	Time associated with input state vector
t_{PEI}	Projected entry interface time
t_{PLS}	Projected landing site time
\underline{v}_D	Velocity at the start of the deorbit maneuver
\underline{v}_{EI}	Entry interface velocity
\underline{v}_0	Input velocity and projected landing site velocity
\underline{v}_{PEI}	Projected entry interface velocity
v_r, v_h	Radial and horizontal components of velocity at entry interface
α_M	Estimated thrust angle at the start of the maneuver
α_{MID}	Thrust angle at the midpoint of the burn
α_{MID0}	Value of α_{MID} from previous iteration cycle
Δd_{ACR}	Increment added to the acceptable crossrange
Δt_F	Time of flight difference between the actual time spent from de-orbit to landing and the orbital time associated with corresponding central angle

Δt_{IP}	Time of flight associated with θ_{IP}
$\Delta \underline{v}$	Maneuver delta velocity
ϵ_0	Auxiliary convergence criterion on α_{MID}
ϵ_1	Fine convergence criterion on α_{MID}
ϵ_2	Rough convergence criterion on α_{MID}
γ_{EI}	Entry interface angle
λ_{LS}	Landing site longitude
ω	Oribtal angular rate
ω_F	Estimated thrust vector's turning rate - inertially defined
ϕ_{LS}	Landing site latitude
μ	Gravitational parameter of the earth
θ	Central angle measured from maneuver centroid
θ_E	Central angle traversed during entry
θ_{IP}	Central angle between the position \underline{r}_D and the projected landing site position
θ_M	Estimated central angle between the start and midpoint of the maneuver
θ_{MEI}	Estimated central angle between the midpoint of the maneuver and the entry interface point

1. INTRODUCTION

The large entry crossrange capability of the Shuttle permits deorbit to a specified landing site to be accomplished with a single maneuver. Since the required velocity change is smallest when no plane change is made, the equations presented here are designed to target the Unified Powered Flight Guidance Routine (Ref. 1) for an in-plane maneuver. The ignition time for this maneuver is selected to satisfy entry interface and landing site constraints with minimum fuel expenditure.

If the Shuttle had no crossrange capability, an in-plane deorbit to a specified landing site would occur only when the landing site, which rotates with the earth, intersects the orbital plane of the vehicle. Assuming the landing site latitude is less than the orbital inclination and neglecting the effects of precession, the landing site will intersect the orbital plane twice every twenty-four hours. The time difference between these two intersections is, in general, not twelve hours. In the case when the landing site latitude is equal to the orbital inclination there will be only one intersection every twenty-four hours.

Since the Shuttle has a large crossrange capability, deorbit can occur whenever the angle between the landing site vector and the orbital plane is less than approximately 20 deg. In general, there will be two sets of opportunities every twenty-four hours. Within each set, there may be several deorbit opportunities occurring on consecutive orbits with varying crossrange requirements. When the latitude of the landing site approaches the inclination of the orbit, these two sets merge to become one. If the landing site latitude is greater than the orbital inclination, the landing site may still fall within the crossrange capability of the vehicle. Based on these considerations, this routine has been designed to step through successive solutions, allowing the crew to select a particular deorbit opportunity based upon entry crossrange, time-to-ignition, required velocity change, landing site lighting conditions, urgency of the return, etc.

The deorbit targeting program is divided into two sections. The first section establishes an initial guess of the landing time based on updating the vehicle in its orbit until its position coincides with the landing site position projected into the plane of the orbit. If the crossrange at this point is not acceptable, the vehicle is updated through successive orbital periods until an acceptable crossrange distance is attained. The second section utilizes the Unified Powered Flight Guidance (UPFG) routine - which is based on velocity-to-be-gained and Linear Tangent Guidance concepts - in order to approximate the effects of the finite deorbit maneuver. This is necessary as the anticipated thrust/weight ratio for the Shuttle during deorbit using a single OHMS engine is 0.025, resulting in long burn arcs. The UPFG routine is called in an iterative loop which searches for the minimum fuel deorbit trajectory.

The desired entry interface conditions (at 400,000 ft) are assumed specified by the relationship

$$v_r = c_1 + c_2 v_h$$

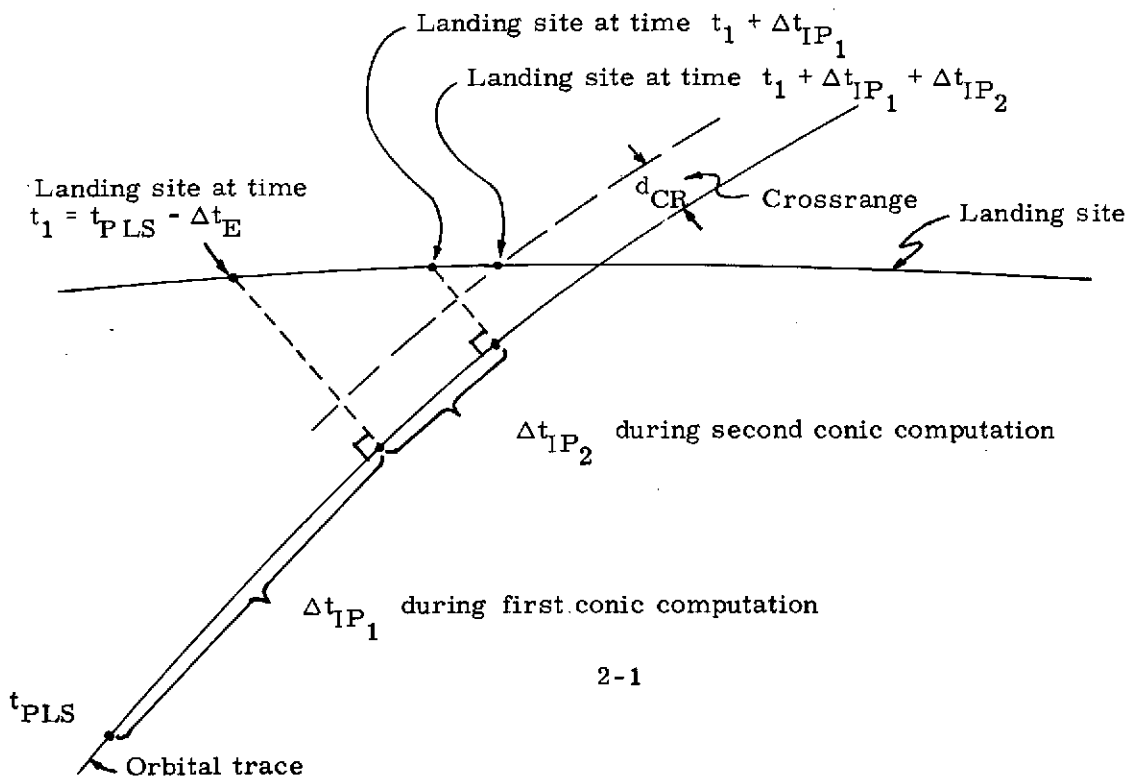
where v_r and v_h are the radial and horizontal components of velocity at the entry interface point and c_1 and c_2 are referred to as the entry interface parameters. This condition is approximately equivalent to a linear relationship between the entry interface angle and velocity. The flight time and range between entry interface and the landing site are assumed to be functionalized in terms of the entry interface flight path angle.

2. FUNCTIONAL FLOW DIAGRAM

A functional flow diagram presenting the basic approach to the deorbit targeting problem is presented in Figure 1. In addition to the vehicle's state vector, the major inputs are landing site location (latitude and longitude), entry interface parameters, earliest desired time of landing and maximum crossrange.

The first section in the deorbit targeting program is to select the earliest landing time which results in an acceptable crossrange. This step is computed using the constraint that the vehicle must arrive above the in-plane projection of the landing site at approximately the same time as was assumed in determining the location of the landing site (which rotates with the earth). In this first step, an estimate of the difference in the time flight between (1) the actual time spent from deorbit to landing and (2) the orbital time associated with the corresponding central angle is utilized. This estimate Δt_E can be represented by a constant as the following steps in the program will compensate for any errors due to this assumption.

To accomplish the first step, the state vector is precision updated to the time t_{PLS} (initially set approximately equal to the desired earliest time of landing). After obtaining the landing site's inertial position based on the time t_{PLS} minus Δt_E , the time Δt_{IP} associated with a conic update of the state vector to a point colinear with the projection of the landing site into the orbital plane is computed. A new estimate of the landing time is now obtained by adding the time Δt_{IP} to the previous landing time. After precision updating the trajectory to the time t_{PLS} plus Δt_{IP} , another calculation of Δt_{IP} is made. Using this Δt_{IP} in a new calculation of the landing time, the above constraint is assumed satisfied. This procedure is illustrated in the following sketch.



If the crossrange d_{CR} computed by the above procedure is not acceptable, the landing time is increased by an orbital period and the above procedure is repeated - with the exception that the second conic update is bypassed - to establish a new crossrange. This process is repeated until an acceptable crossrange is attained.

The second section starts with a computation of an estimated deorbit time and an entry interface position. Following a conic update of the state vector to the deorbit time, an approximate computation of the optimum-inertially defined-turning rate for the thrust direction during the burn is made. The Unified Powered Flight Guidance Routine is next called to compute the variable α_{MID} . This variable represents the approximate direction of the thrust vector at the midpoint of the maneuver, measured with respect to the local horizontal direction. It has been shown (Refs. 2-6) that a burn arc which utilizes a thrust direction which rotates at a constant inertial rate and which results in a α_{MID} value of zero represents an approximate fuel optimum maneuver. The fuel optimum deorbit trajectory can therefore be computed by iteratively varying the time of the deorbit maneuver until α_{MID} is driven to zero. This is accomplished using the Newton-Raphson iterative technique incorporated in the ITER subroutine (Ref. 7). The iteration is accomplished in two phases. In the first phase, the entry interface position and landing time are held fixed while the orbit is conically updated to the ignition point on each iteration cycle. In the second phase - when convergence is near - the entry interface point is computed based on the latest estimate of the landing time and the orbit is precision updated to the ignition point on each iteration cycle. During this phase, the UPFG routine computes a deorbit maneuver based on a precision update of the trajectory from the end of the burn to the entry interface point.*

* Ref. 1, containing the description of the UPFG routine, does not presently allow for this precision updating mode. It will, however, be included in a future update of this reference.

DEORBIT TARGETING

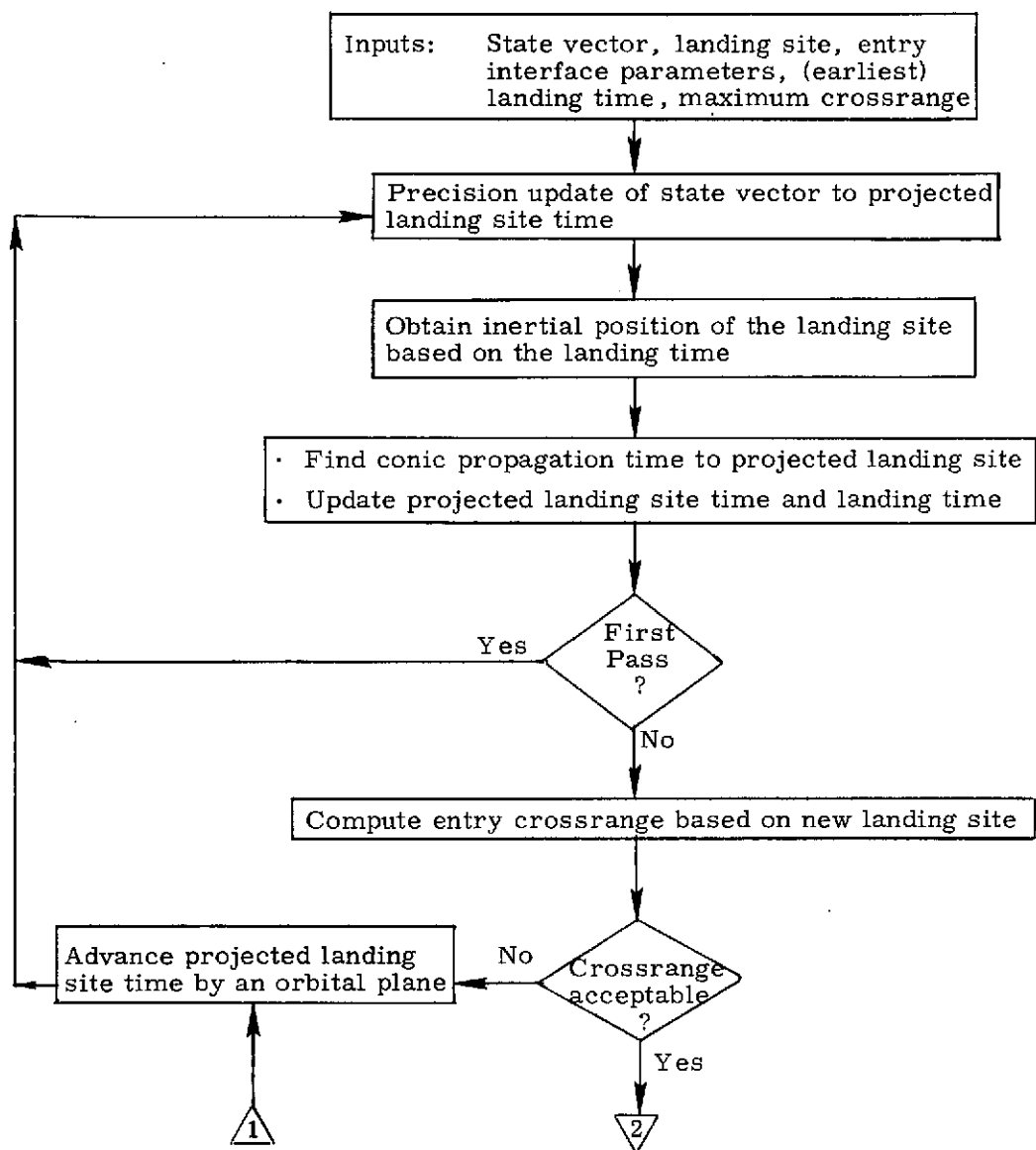


Figure 1a. Functional Flow Diagram

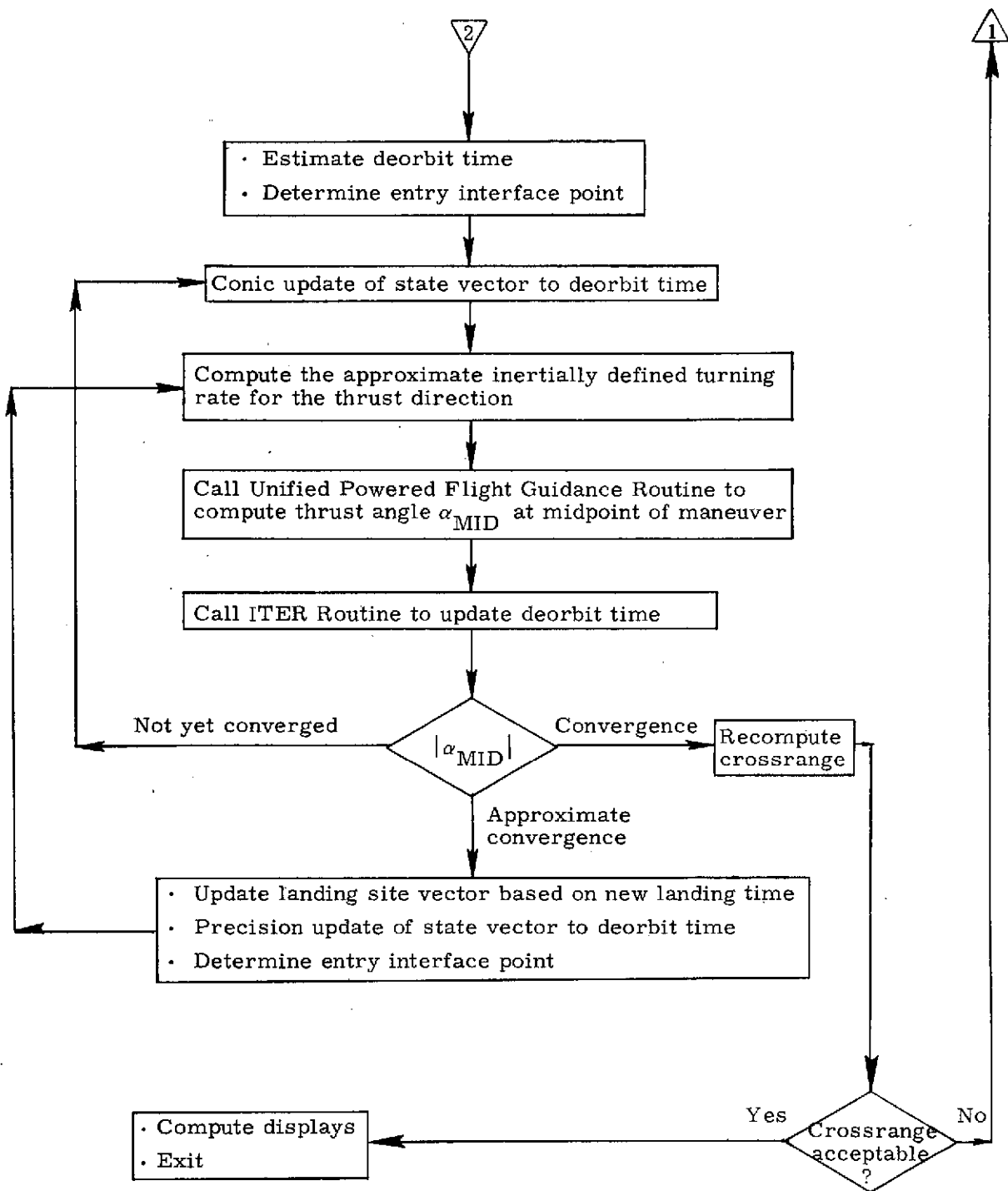


Figure 1b. Functional Flow Diagram

3. INPUT AND OUTPUT VARIABLES

The inputs to the deorbit targeting program are:

$\underline{r}_0, \underline{v}_0$	State vector
t_0	Time associated with $\underline{r}_0, \underline{v}_0$
t_{ETL}	Earliest desired time of landing
t_{LTL}	Latest desired time of landing
m	Estimated vehicle mass
$s_{OMS, 1}$	Number of orbital maneuvering system engines
ϕ_{LS}	Landing site latitude
λ_{LS}	Landing site longitude
d_{ACR}	Maximum acceptable crossrange distance

The output variables are:

t_{ig}	Ignition time
t_{EI}	Time of arrival at the offset target vector
$\Delta \underline{v}$	Maneuver $\Delta \underline{v}$
\underline{r}_{OF}	Offset target vector
n_{rev}	Integral number of revolutions
\underline{i}_N	Unit normal to transfer plane in direction of angular momentum vector
s_{soln}	Lambert solution switch

4. DESCRIPTION OF EQUATIONS

The majority of the deorbit targeting program consists of calls to other routines and simple logical operations, interspersed with some elementary equations. Those operations which are not self evident in terms of the functional flow description and the detailed flow diagram are discussed below.

4.1 Computation of θ_{IP}

The angle between the position vector \underline{r}_0 specified at the projected landing site time t_{PLS} and the projected landing site vector \underline{i}_{LSP} is defined as θ_{IP} . Whenever the crossrange computed in the first section of the deorbit targeting program exceeds the maximum acceptable crossrange, the vehicle's state vector is updated through one orbital period in an attempt to establish an acceptable crossrange. During this interval of time, the inertial position of the landing site changes (due to the rotation of the earth), resulting in an in-plane projection of the landing site which either proceeds or lags the updated state vector. An upper limit on this difference (θ_{IP}) can be established as $\pm 30^\circ$. When the rotational direction of the orbit is opposite to the rotational direction of the earth, this difference will be a negative quantity. Hence, θ_{IP} can be computed as an angle between the limits of -30° and 330° .

In order to make the first computation in Section 1 compatible with subsequent computations, the state vector is initially advanced by one-twelfth of an orbital period (approximately equivalent to 30°) beyond the earliest desired time of landing t_{ETL} .

4.2 Computation of ω_F

Based on the primer vector theory, Refs. 2, 8 and 9, the thrust direction α during an optimum burn must be specified by

$$\tan \alpha = -\sin \theta / (c_3 + 2 \cos \theta) \quad (4.1)$$

θ is the angle from the burn centroid to the point where α is desired. This formulation assumes that the burn occurs under near circular orbital conditions with an inertially defined-constant turning rate maneuver. The constant c_3 can be obtained from the entry interface constraint that the primer vector must be perpendicular to the entry interface constraint line, whose slope is given by (see equation in Section 1)

$$d v_r / d v_h = c_2 \quad (4.2)$$

The desired direction for the primer vector is

$$\alpha_P = -[\tan^{-1}(c_2) + \pi/2] \quad (4.3)$$

As the thrust direction coincides with the direction of the primer vector, Eqs. (4.1) and (4.2) can be combined with the result

$$c_3 = -2 \cos \theta_{MEI} - c_2 \sin \theta_{MEI} \quad (4.4)$$

where θ_{MEI} is the angle between the burn centroid and the entry interface point.

Equation (4.1) now defines the optimum thrust angle as a function of θ , θ_{MEI} and c_2 . Using a central angle θ_M which extends from the centroid to the beginning of the maneuver (θ_M is negative), the thrust direction α_M at the start of the maneuver can be computed. As the thrust direction at the burn centroid should be zero (see Eq. (4.1)), the inertially defined turning rate ω_F for the thrust direction is obtained by noting that the thrust vector must be rotated through both the angle α_M and θ_M

$$\omega_F = -2(\alpha_M + \theta_M)/t_B \quad (4.5)$$

where t_B is the estimated burn time.

The above computations are performed once for each iterative cycle in the second section of the program. Initially, ω_F will be only approximately correct due to an inaccurate estimate of $\Delta \underline{v}$. As the iteration converges to an acceptable value of α_{MID} , the computation of ω_F should become stable and sufficiently accurate (the computation of α_{MID} is not very sensitive to changes in ω_F so the approximation involved in the computation of ω_F are inconsequential).

5. DETAILED FLOW DIAGRAM

This section contains detailed flow diagrams of the deorbit targeting routine.

Each input and output variable in the routine and subroutine call statements can be followed by a symbol in brackets. This symbol identifies the notation for the corresponding variable in the detailed description and flow diagrams of the called routine. When identical notation is used, the bracketed symbol is omitted.

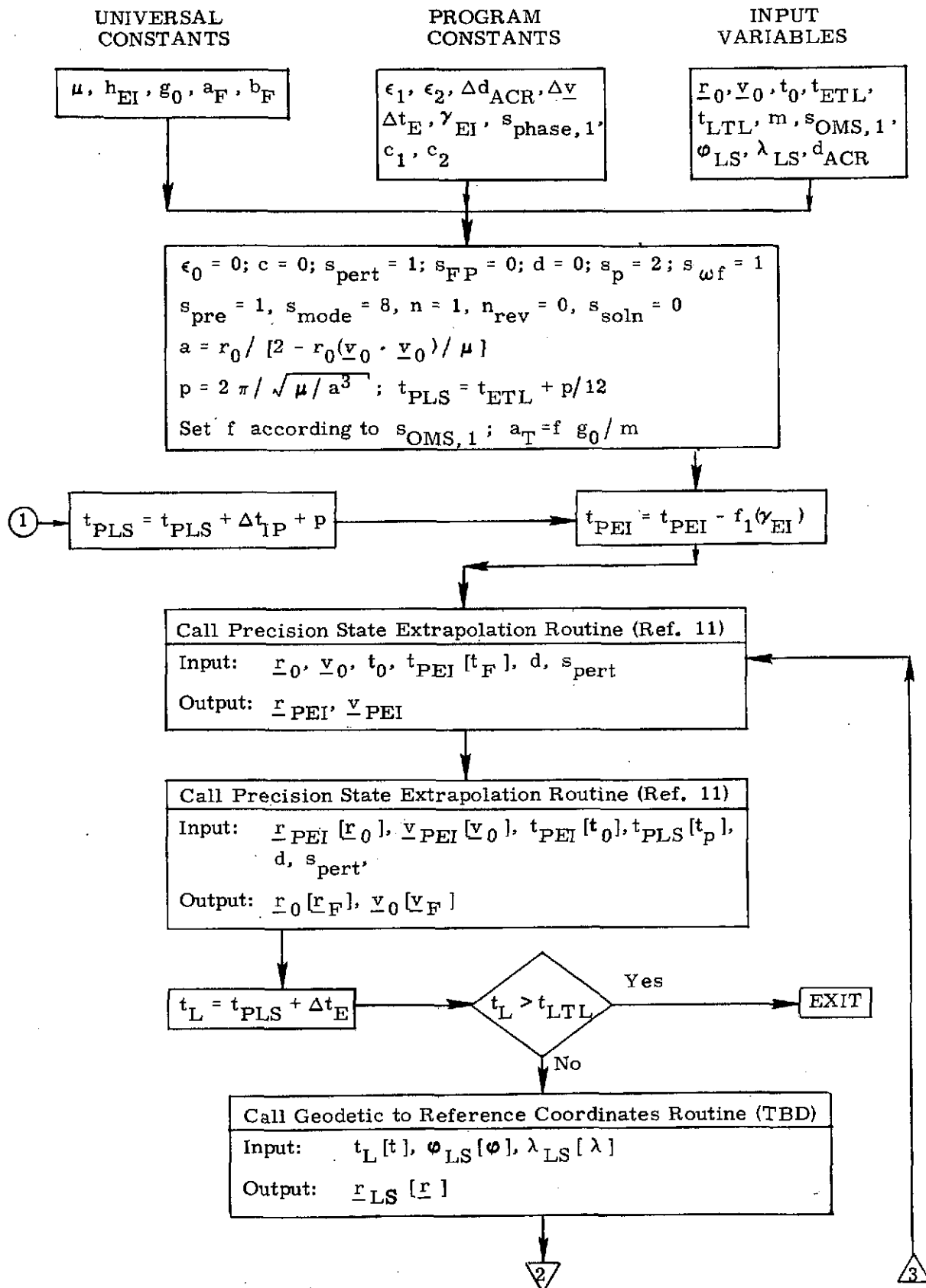


Figure 2a. Detailed Flow Diagram

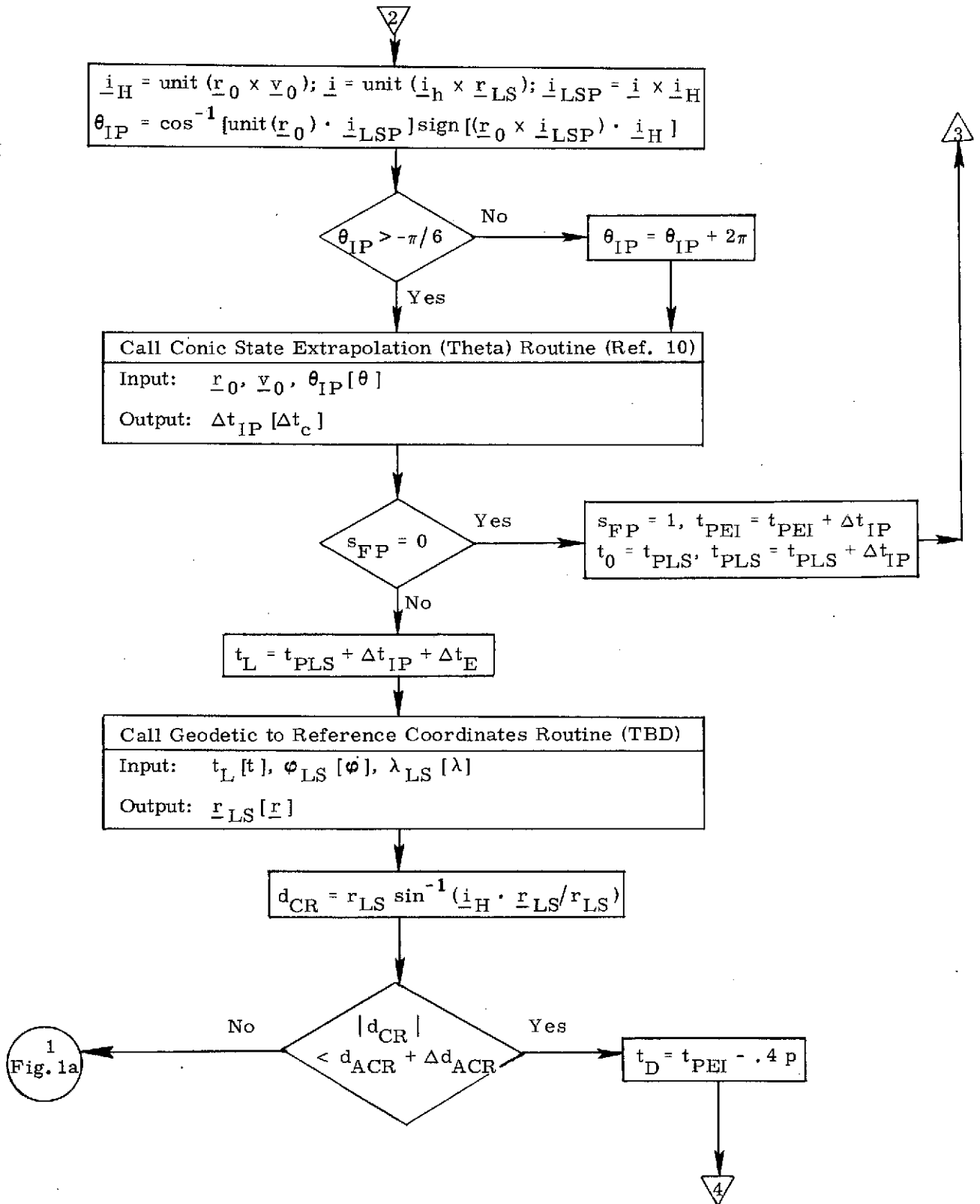


Figure 2b. Detailed Flow Diagram

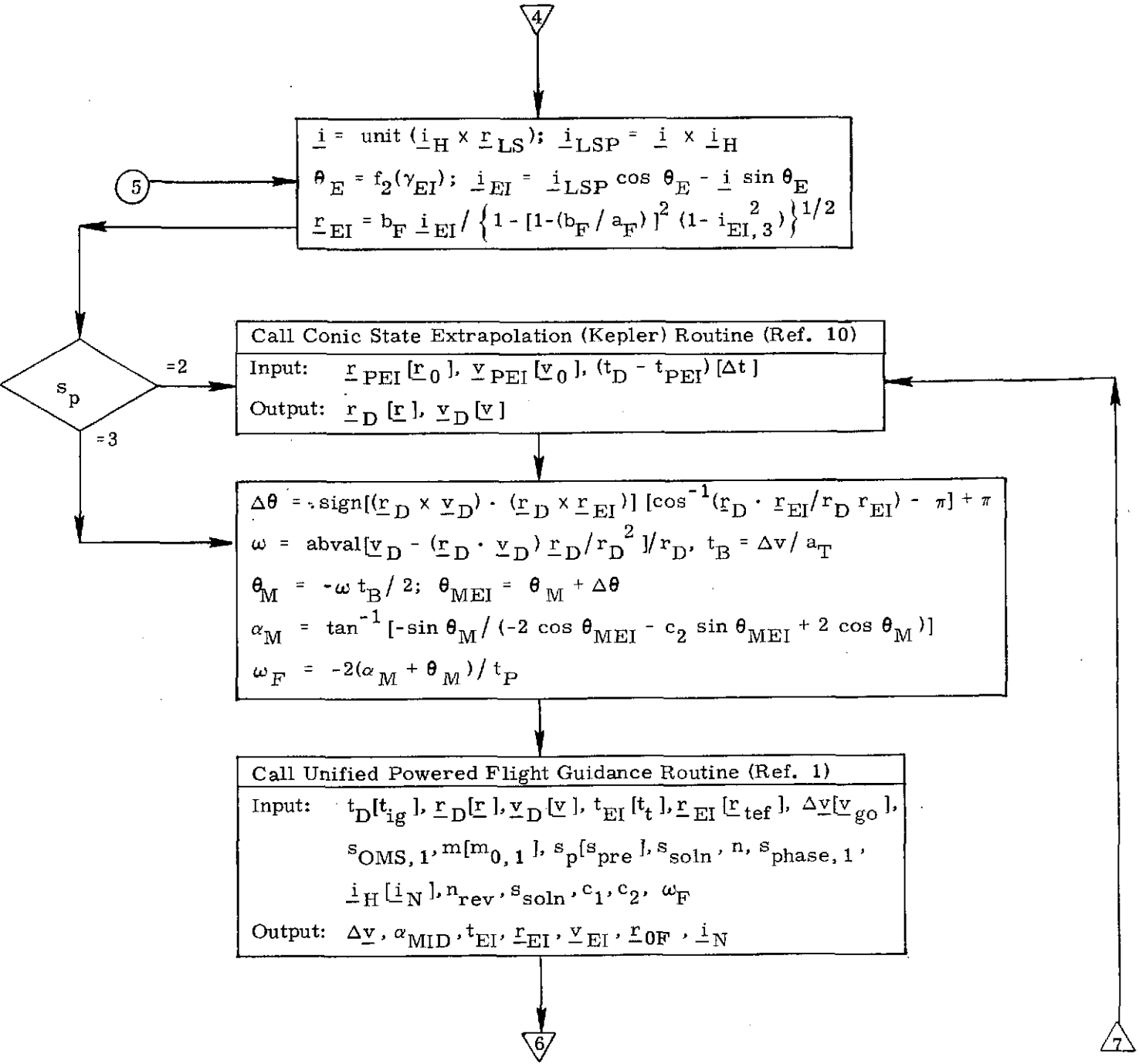


Figure 2c. Detailed Flow Diagram

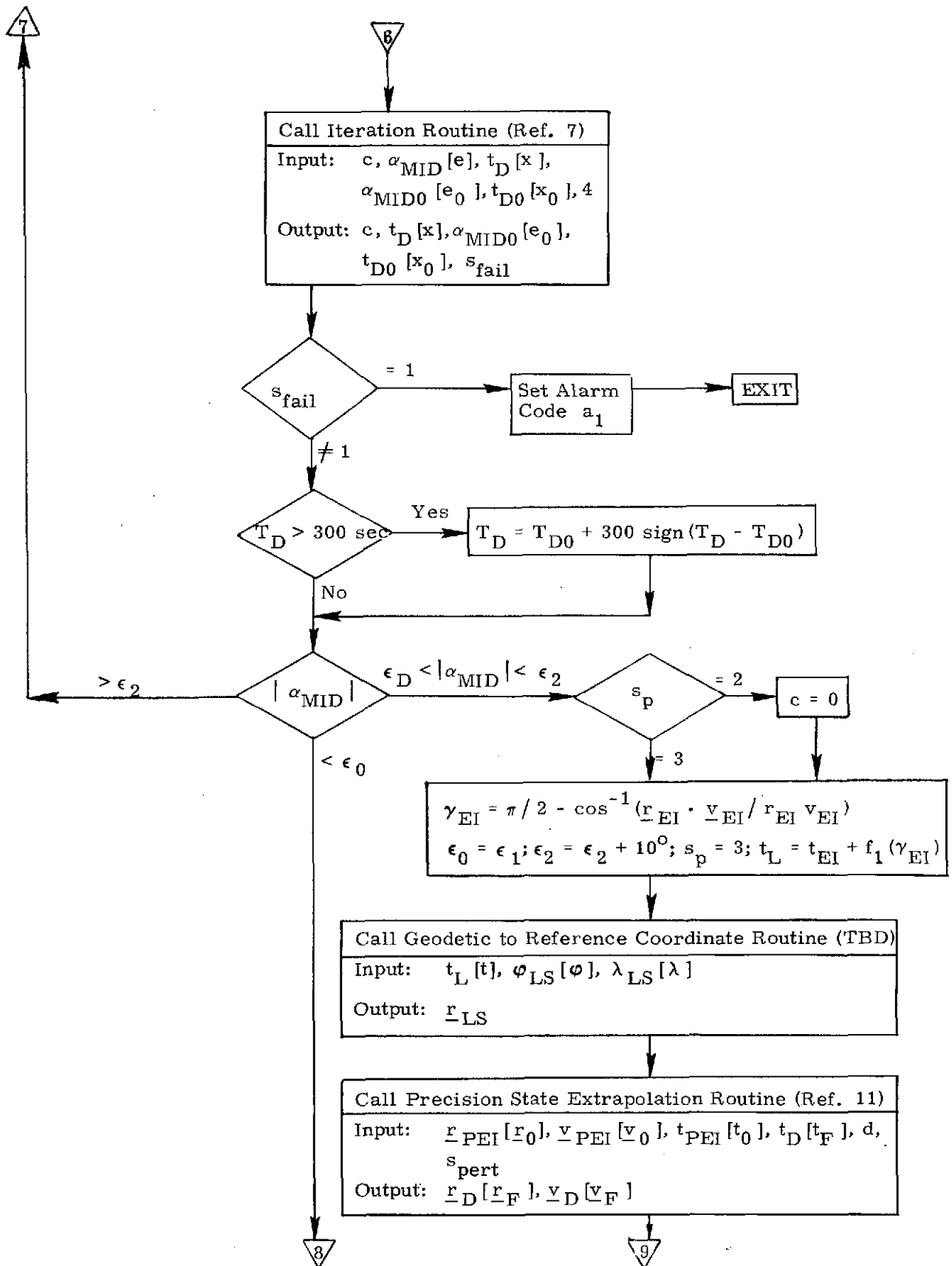


Figure 2d. Detailed Flow Diagram

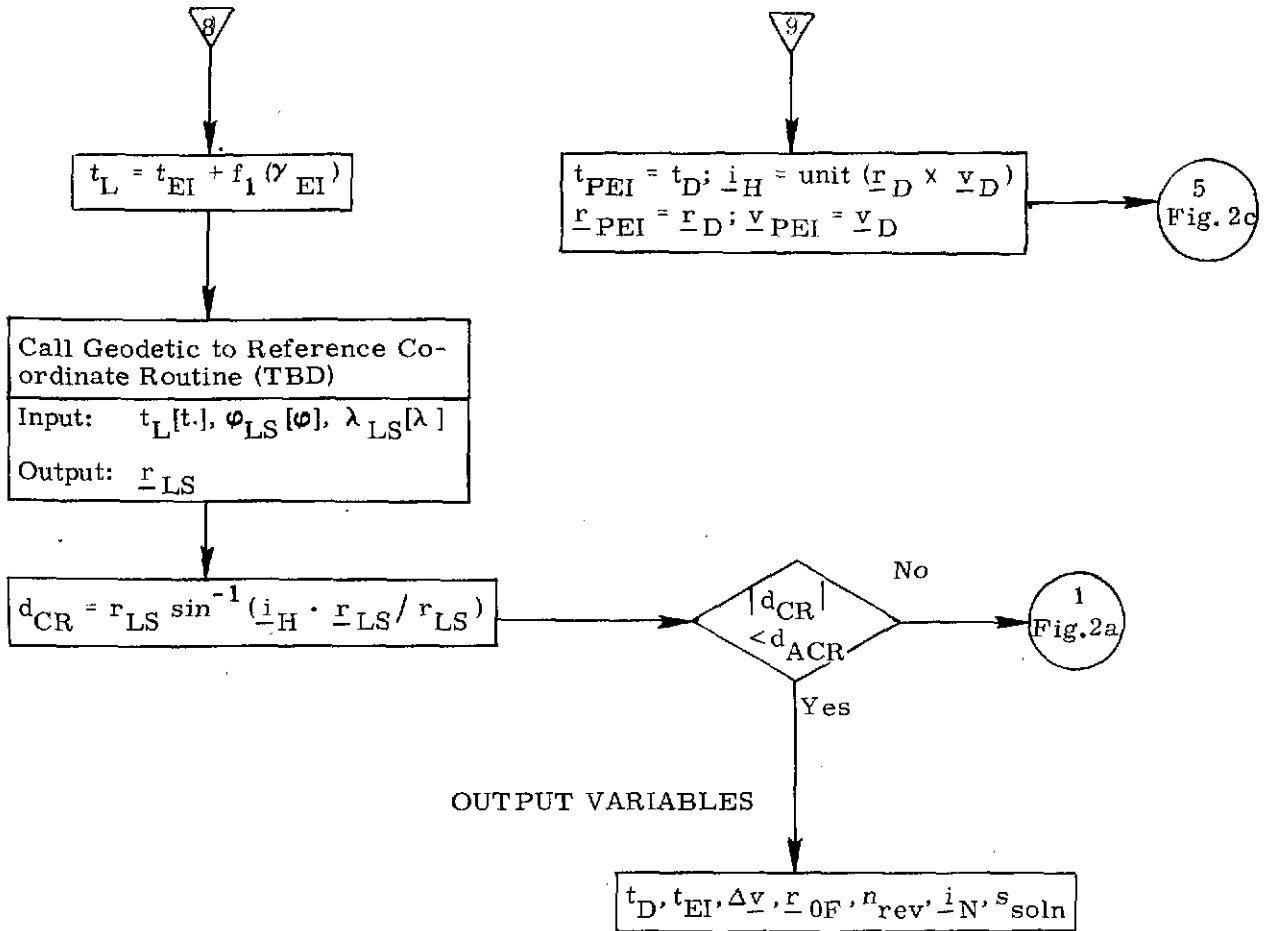


Figure 2e. Detailed Flow Diagram

6. SUPPLEMENTARY INFORMATION

The deorbit targeting technique presented here requires long term state vector extrapolation to select a deorbit opportunity several revolutions later. The accuracy of this extrapolation is dependent upon accurate knowledge of the current state vector. Any errors due to imperfect navigation will tend to be magnified by the long term extrapolation. Fortunately, the out-of-plane component of error tends to oscillate, and can be expected to remain below about 500 ft. Consequently, the prediction of crossrange for a deorbit opportunity several revolutions later is not significantly affected by the expected state vector error. Mission planning functions, which are sensitive to crossrange requirements, can be carried out without being significantly affected by the navigation error.

The in-plane component of state vector error does increase during long term extrapolation, at a rate of about 1000 ft per revolution. Therefore the targeting should be repeated during the revolution prior to the deorbit maneuver, taking advantage of more precise knowledge of the vehicle state vector.

The effect of different azimuths on the entry phase has not been considered in this design. Since the crossrange capability of the vehicle is dependent on azimuth, and thus may be larger in one direction than the other, this should be considered in the acceptable crossrange criterion.

The equations for the determination of the time and range from entry interface to landing are not yet available. Additional analysis in the area of entry guidance should allow the functionalizations of these parameters in terms of the entry interface flight path angle.

The deorbit targeting equations presented here are designed to target a single minimum fuel maneuver which satisfies entry interface and landing site constraints. Since deorbit is the final major maneuver, it may be logical to use all the remaining fuel to either effect a faster return, to reduce the entry crossrange requirement or to decrease the deterioration of the heat shield (by lowering the entry interface velocity). Various methods for accomplishing these goals may be used, including thrusting out-of-plane, using multiple maneuvers to place the vehicle in a phasing orbit prior to the deorbit maneuver and minimizing the entry interface velocity in place of minimizing the fuel. For the most part, these modifications to the deorbit targeting would be superimposed on the logical structure herein contained.

Various empirical studies were undertaken to verify the new deorbit targeting logic. These studies are covered in Refs. 2-6 and include data for circular orbits between altitudes of 70 n. mi. and 500 n. mi. and for a 100 x 270 n. mi. elliptical orbit.

REFERENCES

1. Brown, D., Higgins, J., Brand, T., "Unified Orbiter Powered Flight Guidance", Space Shuttle GN&C Equation Document No. 24, Draper Laboratory, June 1973.
2. Tempelman, W., "A Survey of Fuel Optimum Impulsive and Near Fuel Optimum Finite Thrust Maneuvers for Deorbits from Circular Orbits and a 100 x 270 n. mi. Elliptical Orbit", Draper Laboratory, 23A STS Memo No. 28-73, 29 March 1973.
3. Tempelman, W., "Deorbit Trajectories From a 100 x 270 n. mi. Elliptical Orbit Based on Fixed Deorbit Position", Draper Laboratory, 23A STS Memo No. 31-73, 6 April 1973.
4. Tempelman, W., "A Survey of Deorbit Trajectories Using a Target Line Constraint", Draper Laboratory, 23A STS Memo No. 34-73, 23 April 1973.
5. Tempelman, W., "Deorbit Targeting Using the Unified Powered Flight Guidance Program", Draper Laboratory, 23A STS Memo No. 37-73, 27 April 1973.
6. Tempelman, W., "Comparison Between Predicted Deorbit Targeted Maneuvers and the Actual Maneuvers", Draper Laboratory, 23A STS Memo No. 40-73, 8 May 1973.
7. Tempelman, W., "Rendezvous Targeting", Space Shuttle GN&C Equation Document No. 7, Rev. 2, Draper Laboratory, February 1972.
8. Brown, D., "Thrust Direction Turning Rate for Large Central Angle Shuttle Deorbit Burns", Draper Laboratory, 23A STS Memo No. 55-73, 15 June 1973. (to be published)
9. Lawden, D., "Optimal Trajectories for Space Navigation", Butterworths, London, 1963, p. 96.
10. Shepperd, S., Robertson, W., "Conic State Extrapolation", Space Shuttle GN&C Equation Document No. 25, Draper Laboratory, June 1973, (to be published).
11. Robertson, W., "Precision State and Filter Weighting Matrix Extrapolation", Space Shuttle GN&C Equation Document No. 4, Rev. 3, Draper Laboratory, October 1972.